Chinese Chemical Letters 32 (2021) 3109–3112

Contents lists available at ScienceDirect

Chinese Chemical Letters

journal homepage: www.elsevier.com/locate/cclet

Communication

Dual-functional hydrogen-bonded organic frameworks for aniline and ultraviolet sensitive detection

Zhijun Ke, Kexin Chen, Zhenzhen Li, Jie Huang, Zizhu Yao, Wen Dai, Xiaofan Wang, Chulong Liu*, Shengchang Xiang, Zhangjing Zhang*

Fujian Provincial Key Laboratory of Polymer Materials, College of Chemistry and Materials Science, Fujian Normal University, Fuzhou 350007, China

ARTICLE INFO

Article history:
Received 17 January 2021
Received in revised form 26 February 2021
Accepted 17 March 2021
Available online 19 March 2021

Keywords:
Hydrogen-bonded organic frameworks (HOFs)
Dual-function
Aniline detection
Ultraviolet detection
Sensitive

ABSTRACT

A novel hydrogen-bonded organic frameworks (HOFs) **FJU-200** has been constructed from *N,N'*-bis(5-isophthalic acid)naphthalimide (H_4L). **FJU-200** has a good dual-function of aniline and ultraviolet detection. **FJU-200** is the first case of HOF with dual sensing of visual color changes and photoluminescence quenching for aniline detection, and the detection limit of aniline can reach 5.5×10^{-4} mol/L. Under ultraviolet **FJU-200** will rapidly change from light yellow to rustic brown, which makes it possible to use **FJU-200** to achieve minute-level ultraviolet detection. Moreover, for more convenient use, **FJU-200** test papers are prepared. Using them, convenient and fast aniline or ultraviolet detection can be realized. The single-crystal X-ray structures show that compared with the original **FJU-200**, both **$PhNH_2$@FJU-200** and **UV-FJU-200** have larger pore sizes, and the dihedral angles of the H_2L^{2-} in framework has been changed.

As a typical aromatic amine, aniline is an indispensable chemical precursor, and is widely applied in rubber industries [1], dyes intermediates [2], pharmaceuticals [3], and other fields [4]. However, aniline is toxic, corrosive, difficult to handle, and is easily absorbed subcutaneously and endangers life, even at extremely low concentration. So far, the traditional approaches used to detect amines include high-performance liquid chromatography [5], gas chromatography coupled with mass spectrometry [6], fluorometric analysis [7], and cyclic voltammetry [8]. In fact, these methods require expensive instruments, long analysis time, and professional operators, and they are not easily accessible in most cases [9]. Therefore, rapid and efficient detection of aniline is extremely urgent for public security and environmental protection.

In this regard, porous crystalline chemical sensors have attracted great interest due to their fast, reversible and recyclable sensing capabilities [10–13]. Among them, hydrogen-bonded organic frameworks (HOFs) have attracted many attentions in recent years. The inherent features of hydrogen bond (weak, flexible, poorly directional, and reversible) make HOFs have some intriguing differences compared to zeolites, metal-organic frameworks (MOFs), and covalent organic frameworks (COFs), such as solution processability and characterization, easy purification and healing by simple recrystallization [14]. Recently, many HOFs have been reported with promising applications in gas storage and separation [15–17], proton conduction [18–20], photodynamic therapy [21], heterogeneous catalysis [22], fluorescent sensing [23–25] and so on. However, the exploration of fluorescence sensing of HOFs is still at an early stage and is rarely used to detect aniline.

So far, the study of HOF materials to detect aniline is only one case reported by Zhang's group in 2020 [13]. It is based on analyte–organic linker interaction, in which hydrogen bonds play an important role. Considering that aniline is a good electron donor, we choose an electron-deficient organic linker to construct HOF. *N,N'*-bis(5-isophthalic acid)naphthalimide (H_4L) is a typical electron-deficient and fluorescent linker, which can be used to construct MOFs and as an amine sensor. H_4L is also widely used in optics as a photochromic variable material. Interestingly, it can be used for both naked eye and fluorescence detection. Unfortunately, quite a few metal salts are not environmentally friendly, which often limits the use of MOFs in many conditions [26–28]. Compared with MOFs, HOFs are not restricted by metal salts.

Hence, we synthesized **FJU-200** with H_4L by solvothermal method. Single-crystal X-ray diffraction analysis reveals that **FJU-200** has one-dimensional (1D) pores. When **FJU-200** was immersed in the aniline solution, the single crystal changed from light yellow to deep red, and the transformation from single crystal

* Corresponding authors.
E-mail addresses: liucl@fjnu.edu.cn (C. Liu), zzhang@fjnu.edu.cn (Z. Zhang).

https://doi.org/10.1016/j.cclet.2021.03.043

to single crystal occurred. This is the first case of HOFs, which has visible color changes, photoluminescence quenching dual sensing of aniline. Because the aniline forms a hydrogen bond with the framework of **FJU-200**, the twist of the skeleton is restricted. Moreover, **FJU-200** not only shows a good detection limit but also has a certain specific recognition. The detection limit can reach 5.5×10^{-4} mol/L. In addition, the crystal can be easily deposited on paper, making a simple test paper that can be used for aniline detection. And **FJU-200** is sensitive to ultraviolet light and can achieve minute-level ultraviolet detection.

Single-crystal X-ray diffraction analysis reveals that **FJU-200** crystallizes in the triclinic space group *P-1*. It is composed of H_2L^{2-}, $[NH_2(CH_3)_2]^+$, EtOH and H_2O (Fig. 1a). It is different from the reported three-dimensional HOFs [15,16,29,30]. From the *a*-axis direction, **FJU-200** has a hydrogen-bonded closed ring composed of three different hydrogen bonds. These three hydrogen bonds can be divided into two categories, one of which is the two hydrogen bonds formed by $[NH_2(CH_3)_2]^+$ ion and the adjacent H_2L^{2-} (N—H···O/1.80 Å and 2.01 Å, N—H···O/170.8° and 157.6°), the other is a single hydrogen bond formed by two adjacent H_2L^{2-} (H—O···O/1.79 Å, O—H···O/155.1°) (Fig. 1b). Through the hydrogen bonds formed by adjacent H_2L^{2-}, 1D diamond-shaped pores with a size of 6.50×10.5 Å^2 are constructed, and 1D ribbon structures are formed (Fig. 1b). The hydrogen bond rings are connected each other by a 2.52 Å hydrogen bond formed by dimethylammonium ion and the oxygen atom of 1,3-phthalic acid group in the next layer. The adjacent dimethylammonium ions are bridged by a 2.58 Å hydrogen bond formed by the oxygen atom of the 1,3-phthalic acid group, and the other segment forms a 2.55 Å hydrogen bond with the carbonyl group of H_2L^{2-} in the next layer (Fig. 1c). In this way, the hydrogen-bonded bands are connected to form a two-dimensional (2D) HOF (Fig. 1c). Considering that **FJU-200** has 1D pores, we tried to test N_2 adsorption. Unfortunately, there was almost no N_2 adsorption, and the pores collapsed. At present, acid-base ionic two-component HOFs with permanent pore structures are generally accompanied by interspersed structures or structural characteristics of smaller pore diameters [31–33]. However, **FJU-200** has a large pore size and does not have an interpenetrating structure, and the structural stability is poor. It can easily collapse when **FJU-200** loses the solvent in the framework.

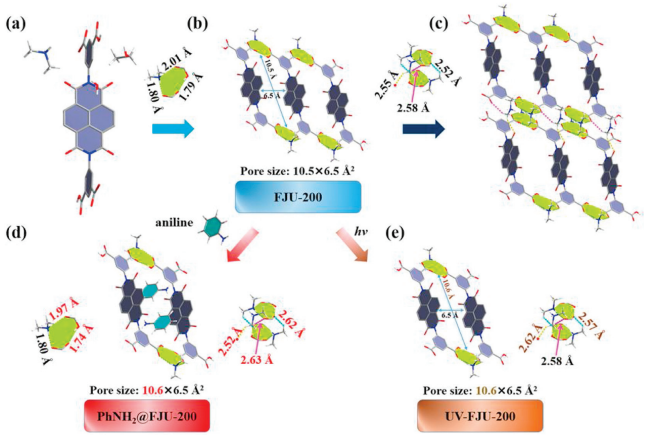

Fig. 1. (a) The main components of **FJU-200** are H_2L^{2-}, $[NH_2(CH_3)_2]^+$, EtOH and H_2O. (b) The 1D structure of **FJU-200**. Three different hydrogen bonds are formed on *b*-axis, forming a hydrogen bond ring. (c) The hydrogen bonds between layers and the 2D structure of **FJU-200**; (d) The 1D structure of **PhNH$_2$@FJU-200**. The hydrogen bond ring has changed significantly, and the pore size has changed from 10.5×6.5 Å^2 to 10.6×6.5 Å^2; (e) The 1D structure of **UV-FJU-200**. The pore size has also changed to 10.6×6.5 Å^2.

Similarly, **PhNH$_2$@FJU-200** crystallizes in the triclinic space group *P-1*. Its asymmetric unit is composed of one-half of H_2L^{2-}, $[NH_2(CH_3)_2]^+$, and aniline. It also forms a 2D HOF. Compared with **FJU-200**, the size of the hydrogen-bonded ring in **PhNH$_2$@FJU-200** has been changed. The hydrogen bond formed by adjacent H_2L^{2-} is strengthened with the length decreased from 1.79 Å to 1.74 Å. In addition, it can be seen from the *a*-axis that the 1D diamond-shaped pores are occupied by aniline, and the pore size increased from 10.5×6.5 Å^2 to 10.6×6.5 Å^2 (Fig. 1d). In the 2D structure formed by **PhNH$_2$@FJU-200**, the hydrogen bond between the hydrogen-bonded bands is weakened with the length increased from 2.52 Å to 2.62 Å, the length of N—H···O hydrogen bond between dimethylammonium ion and the 1,3-phthalic acid group is increased to 2.63 Å, but the hydrogen bond formed at the other end is slightly strengthened with the length decreased to 2.52 Å (Fig. 1d). What's more, from the perspective of the *b*-axis, the dihedral angle between the benzene ring of the 1,3-phthalic acid group and the naphthalene ring of H_2L^{2-} in the middle is 87.7° (Fig. S2c in Supporting information).

UV-FJU-200 also crystallizes in the triclinic space group *P-1*, and forms a 2D HOFs. It is composed of H_2L^{2-}, $[NH_2(CH_3)_2]^+$, EtOH and H_2O. However, we found that there are three obvious differences between **UV-FJU-200** and **FJU-200**. The pore size is slightly larger, increased from 10.5×6.5 Å^2 to 10.6×6.5 Å^2 (Fig. 1e). In the 2D structure formed by **UV-FJU-200**, the hydrogen bond between the hydrogen-bonded bands is weakened with the length increased from 2.52 Å to 2.57 Å, and the length of the hydrogen bond between dimethylammonium ion and the carbonyl group of H_2L^{2-} in the next layer is decreased from 2.55 Å to 2.62 Å (Fig. 1e). In addition, the dihedral angle between the benzene ring and the naphthalene ring of H_2L^{2-} is decreased from 82.5° to 80.5° (Fig. S2b in Supporting information).

The detection of aniline is often affected by other aromatic compounds. Therefore, we performed a specific identification test for **FJU-200**. Some different aromatic compounds such as bromobenzene, toluene, benzaldehyde were tested. Experiments had proved that only aniline had a significant decrease in fluorescence intensity (Fig. 2a). Interestingly, for these aromatic compounds, the color of the crystals becomes darker only when aniline is added (Fig. S3 in Supporting information). Therefore, we further explored the detection of **FJU-200** for aniline in DMF solution. We use the titration method for testing. The results show that it has a good linearity at low concentrations, and the linearity will become worse as the concentration increases, which may be due to self-absorption. The quenching efficiency can be evaluated by the Stern-Volmer (SV) equation: $I_0/I = 1 + K_{sv}[M]$, combined with $3\delta/k$ [34,35], these two equations can be used to calculate the **FJU-200**'s detection of aniline in DMF solution limited to 5.5×10^{-4} mol/L (Fig. 2). The comparison between various luminescence sensors for aniline detection is shown in Table S2 (Supporting information). In addition, the crystal can be easily deposited on paper, so we tried to make a simple test paper that can be used for aniline detection. The results show that **FJU-200** can be made into test paper, which can not only quickly detect aniline, but also the color of the test paper will continue to deepen as the concentration of aniline increases (Fig. 2d).

We found that when **FJU-200** and H_4L dispersed in DMF solution, the emission peaks of the two are the same, which indicates aniline mainly interacts with H_2L^{2-} (Fig. S4 in Supporting information). From the results of single crystal X-ray diffraction, there are significant differences between **FJU-200** and **PhNH$_2$@FJU-200**. First, from the *b*-axis, the dihedral angle of **PhNH$_2$@FJU-200** is 5.2° larger than that of **FJU-200** (Fig. 3a). Second, the aniline forms a hydrogen bond with the skeleton of H_2L^{2-}. This is because aniline is a very good electron donor, and H_4L is a good electron acceptor. When aniline is present in **FJU-200**, the

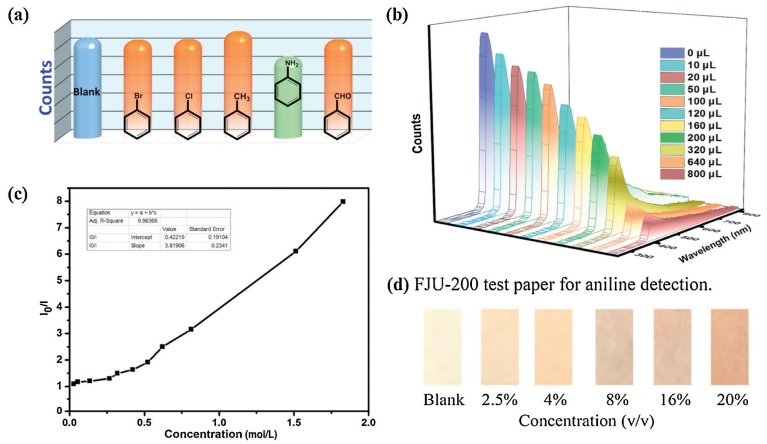

Fig. 2. (a) Fluorescence intensities of different aromatic compounds. The original sample followed by chlorobenzene, bromobenzene, toluene, aniline, and benzaldehyde (0.01 mol/L in DMF). Only aniline exhibited a decrease in fluorescence. (b) The luminescence of **FJU-200** is dispersed in different concentrations of aniline solution. (c) The Stern-Volmer curve of the solubility of I_0/I and aniline of **FJU-200** in DMF suspension. (d) Photos of **FJU-200** test papers used to test different concentrations of aniline solution (v/v).

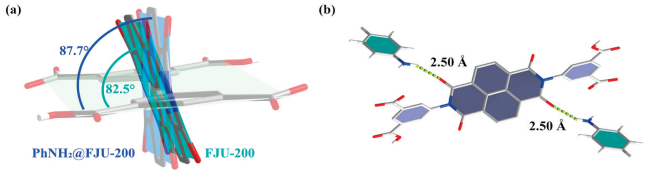

Fig. 3. (a) From the *b*-axis direction, the dihedral angle of the benzene ring and naphthalene ring of **FJU-200** is 82.5°, while that of **PhNH$_2$@FJU-200** is 87.7°. The two dihedral angles differ by 5.2°. (b) Aniline forms a hydrogen bond with the carbonyl group on the **PhNH$_2$@FJU-200** skeleton, with a length of 2.50 Å.

carbonyl group of H_2L^{2-} on the skeleton is a good site, which can form a N—H···O (2.50 Å) hydrogen bond with the amino group of aniline (Fig. 3b). The interactions of the two hydrogen bonds increase the dihedral angle and decrease the overlap of the electron cloud density, which lead the anti-bond orbital energy increased, thereby decreasing the fluorescence.

UV-FJU-200, like **ECUT–HOF-30** [36], is very sensitive to ultraviolet rays. When using ultraviolet light (365 nm) to irradiate **FJU-200** only for 1 min, the crystal changes from light yellow to rustic brown. Since **FJU-200** is sensitive to ultraviolet, we made **FJU-200** into test paper and exposed it to the sun. The test paper changed color after 1 min, and the color became darker after 3 min. These results show that it can be used for the rapid detection of ultraviolet light (Fig. 4). **FJU-200** solid-state UV–vis spectrum display a broad absorption band of about 400 nm corresponds to n-π^* and π-π^* transitions of the aromatic organic part [37]. Remarkably, after irradiation for 1 min, several new additional peaks (607 nm, 711 nm and 784 nm) were generated, which arises from a photo-induced electron-transfer transition. Naphthalene-tetracarboxdiimide (NDI) moiety is known to be redox-active and can generate radicals upon light irradiation [38,39]. This radical generation has been confirmed by the ESR spectra (Fig. 4a). **FJU-200** shows a weak ESR signal at $g = 2.0030$ before irradiation; however, after irradiation the signal gets enhanced. Single crystal X-ray diffraction shows that the **UV-FJU-200** single crystal structure has undergone subtle changes. The single crystal structure of **UV-FJU-200** shows that water molecules and H_2L^{2-} form a lone-pair···π after light exposure was weakened with the length increased from 2.96 Å to 2.97 Å. It plays an important role in the electron transfer electron transfer transition [40–43]. At the same time, we also found that the C—H···O hydrogen bond formed by the carbonyl group and the adjacent dimethylammonium ion

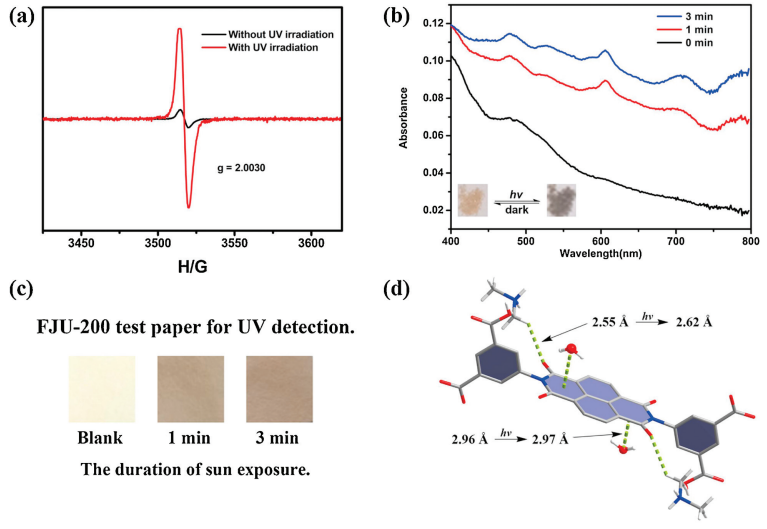

Fig. 4. (a) ESR spectra of **FJU-200** with and without UV irradiation. (b) UV–vis spectra of **FJU-200** under ultraviolet light (365 nm) for 1 min, 3 min. (c) Photos of **FJU-200** test papers in different duration of sun expose (taken in Fuzhou at 2 pm on Nov. 20, 2020, a sunny day). (d) Changes of hydrogen bonds in **FJU-200** after UV irradiation.

also weakened with the length increased from 2.55 Å to 2.62 Å. Under the applied force, the naphthalene ring of H_2L^{2-} was deflected, and the dihedral angle decreased from the original 82.1° to 80.2°. This is the first time that the electronic transition process caused by multiple forces has been observed in the hydrogen-bonded organic framework after ultraviolet light.

In short, we chose the classic fluorescent linker H_4L and synthesized **FJU-200** by hydrothermal method. When **FJU-200** is immersed in aniline solution, the transformation from single crystal to single crystal can occur. Studies have shown that under the synergistic effect of two N—H···O hydrogen bonds, the dihedral angle of H_4L can be changed. In this way, the fluorescence intensity of the crystal can be changed and both naked eye and fluorescent detection can be used. In addition, **FJU-200** is sensitive to ultraviolet and can be used to quickly and conveniently detect ultraviolet. This provides a new way to design HOF materials for rapid detection of aniline and ultraviolet light.

Declaration of competing interest

The authors report no declarations of interest.

Acknowledgments

This work was supported by the National Natural Science Foundation of China (Nos. 21673039, 21573042, 21805039, 21975044, 21971038 and 21922810) and the Fujian Provincial Department of Science and Technology (Nos. 2018J07001 and 2019H6012).

Appendix A. Supplementary data

Supplementary material related to this article can be found, in the online version, at doi:https://doi.org/10.1016/j.cclet.2021.03.043.

References

[1] B.G. Soares, G.S. Amorim, F.G. Souza, M.G. Oliveira, J.E.P. da Silva, Synthetic Met. 156 (2006) 91–98.
[2] A. Grirrane, A. Corma, H. García, Science 322 (2008) 1661.
[3] V. Alagarsamy, V.R. Solomon, K. Dhanabal, Bioorg. Med. Chem. 15 (2007) 235–241.
[4] J.M. Landete, B. de las Rivas, A. Marcobal, R. Muñoz, Int. J. Food Microbiol. 117 (2007) 258–269.
[5] Z. Quan, G. Xie, Q. Peng, et al., Pol. J. Environ. Stud. 25 (2016) 1669–1673.
[6] W.G. Stillwell, M.S. Bryant, J.S. Wishnok, Biomed. Environ. Mass Spectrom. 14 (1987) 221–227.
[7] Y. Zhang, C. Peng, X. Ma, Y. Che, J. Zhao, Chem. Commun. 51 (2015) 15004–15007.
[8] S. Pandey, K.K. Nanda, ACS Sens. 1 (2016) 55–62.
[9] J.J. Liu, Q.T. Que, D. Liu, et al., CrystEngComm 22 (2020) 4124–4129.
[10] M.E. Davis, Nature 417 (2002) 813–821.
[11] Z. Xie, L. Ma, K.E. deKrafft, A. Jin, W. Lin, J. Am. Chem. Soc. 132 (2010) 922–923.
[12] J. Zhang, X. Liu, S. Wu, et al., J. Mater. Chem. 20 (2010) 6453–6459.
[13] B. Wang, R. He, L.H. Xie, et al., J. Am. Chem. Soc. 142 (2020) 12478–12485.
[14] R.B. Lin, Y. He, P. Li, et al., Chem. Soc. Rev. 48 (2019) 1362–1389.
[15] Y. He, S. Xiang, B. Chen, J. Am. Chem. Soc. 133 (2011) 14570–14573.
[16] H. Wang, B. Li, H. Wu, et al., J. Am. Chem. Soc. 137 (2015) 9963–9970.
[17] W. Yang, A. Greenaway, X. Lin, et al., J. Am. Chem. Soc. 132 (2010) 14457–14469.
[18] A. Karmakar, R. Illathvalappil, B. Anothumakkool, et al., Angew. Chem. Int. Ed. 55 (2016) 10667–10671.
[19] G. Xing, T. Yan, S. Das, T. Ben, S. Qiu, Angew. Chem. Int. Ed. 57 (2018) 5345–5349.
[20] W. Yang, F. Yang, T.L. Hu, et al., Cryst. Growth Des. 16 (2016) 5831–5835.
[21] Q. Yin, P. Zhao, R.J. Sa, et al., Angew. Chem. Int. Ed. 57 (2018) 7691–7696.
[22] B. Han, H. Wang, C. Wang, et al., J. Am. Chem. Soc. 141 (2019) 8737–8740.
[23] I. Hisaki, Y. Suzuki, E. Gomez, et al., J. Am. Chem. Soc. 141 (2019) 2111–2121.
[24] Z. Sun, Y. Li, L. Chen, X. Jing, Z. Xie, Cryst. Growth Des. 15 (2015) 542–545.
[25] T. Liu, B. Wang, R. He, et al., Can. J. Chem. 98 (2020) 352–357.
[26] A. Mallick, B. Garai, M.A. Addicoat, et al., Chem. Sci. 6 (2015) 1420–1425.
[27] M. Al Kobaisi, S.V. Bhosale, K. Latham, et al., Chem. Rev. 116 (2016) 11685–11796.
[28] A.M. Rice, C.R. Martin, V.A. Galitskiy, et al., Chem. Rev. 120 (2020) 8790–8813.
[29] Q. Yin, Y.L. Li, L. Li, et al., ACS Appl. Mater. Interfaces 11 (2019) 17823–17827.
[30] H. Wang, H. Wu, J. Kan, et al., J. Mater. Chem. A 5 (2017) 8292–8296.
[31] A. Comotti, S. Bracco, A. Yamamoto, et al., J. Am. Chem. Soc. 136 (2014) 618–621.
[32] J. Lü, C. Perez-Krap, M. Suyetin, et al., J. Am. Chem. Soc. 136 (2014) 12828–12831.
[33] I. Brekalo, D.E. Deliz, L.J. Barbour, et al., Angew. Chem. Int. Ed. 59 (2020) 1997–2002.
[34] L. Liu, Y. Wang, R. Lin, et al., Dalton Trans. 47 (2018) 16190–16196.
[35] Y. Salinas, R. Martínez-Máñez, M.D. Marcos, et al., Chem. Soc. Rev. 41 (2012) 1261–1296.
[36] L. Wang, L. Yang, L. Gong, et al., Chem. Eng. J. 383 (2020) 123117.
[37] Z. Li, J. Guo, F. Xiang, et al., CrystEngComm 20 (2018) 7567–7573.
[38] L. Han, L. Qin, L. Xu, et al., Chem. Commun. 49 (2013) 406–408.
[39] F. Wei, Y. Ye, W. Huang, et al., Inorg. Chem. Commun. 93 (2018) 105–109.
[40] J.J. Liu, Y.J. Hong, Y.F. Guan, et al., Dalton Trans. 44 (2015) 653–658.
[41] J.J. Liu, Z.J. Wang, S.B. Xia, J. Liu, X. Shen, Dye. Pigment. 172 (2020) 107856.
[42] J.Z. Liao, J.F. Chang, L. Meng, et al., Chem. Commun. 53 (2017) 9701–9704.
[43] C. Fu, G.S. Zhang, H.Y. Wang, et al., CrystEngComm 20 (2018) 6821–6827.